

Footprint in fitting $B \rightarrow D$ vector form factor and determination for D -meson leading-twist LCDA

Sheng-Bo Wu,¹ Hai-Jiang Tian,¹ Yin-Long Yang,¹ Wei Cheng,² Hai-Bing Fu,^{1,3,*} and Tao Zhong^{1,3}

¹*Department of Physics, Guizhou Minzu University, Guiyang 550025, P.R.China*

²*School of Science, Chongqing University of Posts and Telecommunications, Chongqing 400065, China*

³*Institute of High Energy Physics, Chinese Academy of Sciences, Beijing 100049, P.R.China*

(Dated: January 7, 2025)

In this paper, we fit the $B \rightarrow D$ vector transition form factor (TFF) by using the data measured by BABAR and Belle Collaborations within Monte Carlo (MC) method. Meanwhile, the $B \rightarrow D$ TFF is also calculated by using the QCD light-cone sum rules approach (LCSRs) within right-handed chiral current correlation function. In which, the D -meson leading-twist light-cone distribution amplitude (LCDA) serves as crucial input parameter is reconstructed with light-cone harmonic oscillator model where its longitudinal behavior primarily determined by the model-free parameter $B_{2;D}$. After matching the TFF with two scenarios from MC and LCSRs, we have $B_{2;D} = 0.17$. Then, we present the curve of D -meson leading-twist LCDA in comparison with other theoretical approaches. Subsequently, the $B \rightarrow D$ TFF $f_+^{BD}(q^2)$ at the large recoil region is $f_+^{BD}(0) = 0.625_{-0.113}^{+0.087}$, which is compared in detail with theoretical estimates and experimental measurements. Furthermore, we calculate the decay width and branching ratio of the Cabibbo-favored semileptonic decays $B \rightarrow D\ell\bar{\nu}_\ell$, which lead to the results $\mathcal{B}(B^0 \rightarrow D^-\ell^+\nu_\ell) = (1.96_{-0.55}^{+0.51}) \times 10^{-2}$ and $\mathcal{B}(B^+ \rightarrow \bar{D}^0\ell^+\nu_\ell) = (2.12_{-0.59}^{+0.55}) \times 10^{-2}$. Finally, we predict the CKM matrix element with two scenarios $|V_{cb}|_{\text{SR}} = 42.97_{-2.57}^{+2.42} \times 10^{-3}$ and $|V_{cb}|_{\text{MC}} = 42.82_{-1.29}^{+1.07} \times 10^{-3}$ from $B^0 \rightarrow D^-\ell^+\nu_\ell$, $|V_{cb}|_{\text{SR}} = 41.93_{-1.05}^{+1.03} \times 10^{-3}$ and $|V_{cb}|_{\text{MC}} = 41.82_{-0.25}^{+0.23} \times 10^{-3}$ from $B^+ \rightarrow \bar{D}^0\ell^+\nu_\ell$ which are in good agreement with theoretical and experimental predictions.

PACS numbers: 12.15.Hh, 13.25.Hw, 14.40.Nd, 11.55.Hx

I. INTRODUCTION

In the Standard Model (SM) framework, the exploration of heavy flavor physics is crucial, which can provide a clean environment to test and perfect the SM, and search for new physics beyond the SM. The semileptonic decay $B \rightarrow D\ell\bar{\nu}_\ell$ is a fascinating process, which can suitably determine the Cabibbo-Kobayashi-Maskawa (CKM) matrix element $|V_{cb}|$ [1–5] and exhibit other interesting observables, intriguing both theorists and experimentalists in physics. At present, there are still non-negligible errors in the SM parameters. For example, in the CKM matrix element of the second row, the uncertainty of $|V_{cb}|$ is the largest, which is 3.4% in comparing with $|V_{cd}|$ and $|V_{cs}|$. Therefore, the relevant calculations still need to continuously improve the measurement accuracy. On the other hand, the hadron form factor which is also known as transition form factor (TFF) is the key component in calculating the semileptonic $B \rightarrow D\ell\bar{\nu}_\ell$ decay process in perturbative QCD theory.

For this point, there have been many experimental groups to study this process. Early in 1997, CLEO Collaboration gave the branching fractions of $\bar{B} \rightarrow D\ell\bar{\nu}$ with $\mathcal{B}(\bar{B}^0 \rightarrow D^+\ell^-\bar{\nu}_\ell) = (1.87 \pm 0.15 \pm 0.32)\%$, $\mathcal{B}(B^- \rightarrow D^0\ell^-\bar{\nu}_\ell) = (1.94 \pm 0.15 \pm 0.34)\%$ [6]. Then they updated $\mathcal{B}(\bar{B}^0 \rightarrow D^+\ell^-\bar{\nu}_\ell) = (2.20 \pm 0.16 \pm 0.19)\%$, $\mathcal{B}(B^- \rightarrow D^0\ell^-\bar{\nu}_\ell) = (2.32 \pm 0.17 \pm 0.20)\%$ by using a sample of $3.3 \times$

10^6 B -meson decays [7]. In 2009, BABAR Collaboration reported $\mathcal{G}(1)|V_{cb}| = (43.0 \pm 1.9 \pm 1.4) \times 10^{-3}$ and branching fractions $\mathcal{B}(B^- \rightarrow D^0\ell^-\bar{\nu}_\ell) = (2.31 \pm 0.08 \pm 0.09)\%$, $\mathcal{B}(\bar{B}^0 \rightarrow D^+\ell^-\bar{\nu}_\ell) = (2.23 \pm 0.11 \pm 0.11)\%$ based on 460 million $B\bar{B}$ events recorded at the $\Upsilon(4S)$ resonance [8]. Furthermore, they updated $|V_{cb}| = (41.09 \pm 1.16) \times 10^{-3}$ by using the entire BABAR $\Upsilon(4S)$ data in 2023 [9]. In 2002, Belle Collaboration presented branching fraction $\mathcal{B}(\bar{B}^0 \rightarrow D^+\ell^-\bar{\nu}) = (2.13 \pm 0.12 \pm 0.39)\%$ and $B \rightarrow D$ TFF at the point of zero recoil with CKM matrix element $|V_{cb}|F_D(1) = (4.11 \pm 0.41 \pm 0.52) \times 10^{-2}$ [10]. Moreover, they update the measurement $\mathcal{G}(1) = 1.0541 \pm 0.0083$, $\mathcal{B}(\bar{B}^0 \rightarrow D^+\ell^-\bar{\nu}) = (2.31 \pm 0.03(\text{stat}) \pm 0.11(\text{syst}))\%$, $|V_{cb}| = (40.83 \pm 1.13) \times 10^{-3}$ by using the decay $B \rightarrow D\ell\nu_\ell$ based on 711 fb^{-1} of $e^+e^- \rightarrow \Upsilon(4S)$ data in 2015 [11]. Moreover, in 2022, the Belle-II Collaboration once again update their research on the semileptonic decays $B \rightarrow D\ell\nu_\ell$, based on Belle-II data from 2019-2021, corresponding to an integrated luminosity of 189.2 fb^{-1} with $|V_{cb}| = (38.28 \pm 1.16) \times 10^{-3}$ [12].

On the theoretical side, there are various approaches to study the semileptonic decay $B \rightarrow D\ell\bar{\nu}_\ell$, such as the perturbative QCD (pQCD) [13–15], the QCD light-cone sum rule (LCSRs) [16–22] and the lattice QCD (LQCD) [23–30]. Different approaches are suitable in different squared momentum transfer q^2 -region when calculating $B \rightarrow D$ TFF. Combining them may offer better results [31, 32]. The pQCD method can offer a more suitable contribution in the large recoil region, while the LQCD approach is more appropriate for soft regions with large q^2 . The QCD LCSRs approach involves both the hard and the

* fuhb@gzmu.edu.cn

soft contributions below $\sim 8 \text{ GeV}^2$. The following discusses some of the theoretical calculations. For pQCD method, the TFF at large recoil region and branching fraction are $f_+^{BD}(0) = 0.52_{-0.10}^{+0.12}$, $\mathcal{B}(\bar{B}^0 \rightarrow D^+ \ell^- \bar{\nu}_\ell) = (2.03_{-0.70}^{+0.92}) \times 10^{-2}$, and $\mathcal{B}(B^- \rightarrow D^0 \ell^- \bar{\nu}_\ell) = (2.19_{-0.76}^{+0.99}) \times 10^{-2}$ [13]. From the LCSR approach, the situation are $f_+^{BD}(0) = 0.552 \pm 0.216$ and $|V_{cb}| = 40.2_{-0.5}^{+0.6} \times 10^{-3}$ [21]. The LQCD predictions are $f_+^{BD}(0) = 0.672 \pm 0.027$ and $|V_{cb}| = (39.6 \pm 1.7 \pm 0.2) \times 10^{-3}$ [24]. There exist large a gap for the vector TFF from different methods, which leads to the first motivation for this paper. Recently, the large momentum effective theory (LaMET) is integrated with the Lattice techniques to explore the B -meson light-cone distribution amplitude (LCDA) [33, 34]. It is known that the B -meson LCDA assumes a highly significant role in the investigation of B -meson decay phenomena, especially for the soft-collinear effective theory (SCET) [35, 36]. When dealing with the D -meson LCDA, it will encounter some problems due to the smaller mass of D -meson which is close to Λ_{QCD} . A determined D -meson LCDA will be helpful to study the D -meson related decay processes which lead to the second motivation of this paper.

Based on the above discussion, the process is worth to be studied due to the result difference between the experimental measurements and the theoretical calculations. The accurate measurement of $|V_{cb}|$ depends heavily on reliable $B \rightarrow D$ TFF. The Belle and BABAR Collaborations continuously detect the $B \rightarrow D \ell \nu$ process and give a large amount of TFF information that can be referenced. The Monte Carlo (MC) method allows us to effectively use a set of data on the $B \rightarrow D$ TFF for related calculations. One can fit the TFF data set provided by multiple experimental groups using the MC method and apply the fitted results to comment the relevant decay widths, branching fractions of semileptonic decay $B \rightarrow D \ell \bar{\nu}_\ell$, and the CKM matrix element $|V_{cb}|$, with the aim of comparing both experimental and theoretical results.

After obtaining the resultant fitted data, we shall adopt the improved QCD LCSRs approach (*i.e.* starting from the chiral correlation function) to calculate the $B \rightarrow D$ TFF, enabling the comparison between experimental and theoretical results. Meanwhile, the D -meson leading-twist LCDA, which serve as a crucial parameter input, is also considered. The D -meson leading-twist LCDA is the dominant contribution, while the most uncertain twist-3 contribution can be suitably eliminated by the chiral correlation function. Moreover, as the twist-4 contribution is small in LCSRs, one can furnish a good platform to test the D -meson leading-twist LCDA based on the obtained $B \rightarrow D$ TFF. Therefore, we present a model for D -meson leading-twist LCDA $\phi_{2,D}(x, \mu_0^2)$, which is constructed by the Brodsky-Huang-Lepage (BHL) prescription [37–44] together with the Wigner-Melosh rotation effect [45–47]. In this work, the model will incorporate three unknown parameters to appropriately describe the behavior of the D -meson leading-twist LCDA, which will be discussed

in the next section. Among these unknown parameters, there is a free parameter $B_{2,D}$ that governs the longitudinal behavior of the LCDA. To present a better behavior of the D -meson leading-twist LCDA, as proposed in this manuscript, the free parameter $B_{2,D}$ is adjusted within an appropriate range by matching the fitted $B \rightarrow D$ TFF obtained from the MC technique. Based on this, the improved LCSRs TFF can be more effectively applied in calculations. Further study, using the $B \rightarrow D$ TFFs obtained from the MC and LCSRs techniques, will allow one to assess their behaviors and corresponding physical observables, thereby demonstrating the model's applicability to the D -meson leading-twist LCDA.

The remaining parts of paper are organized as follows: In Section II, we present the theoretical framework for studying the $B \rightarrow D$ semileptonic processes. Section III is dedicated to the numerical analysis, where we provide the transition form factors, decay branching ratios, and predict the numerical results for the CKM matrix elements. Section IV is reserved for a summary.

II. THEORETICAL FRAMEWORK

The $B \rightarrow D$ TFFs $f_+^{BD}(q^2)$ and $\mathcal{G}(w)$ are defined from the basic matrix element which have the following form

$$\begin{aligned} \langle D(p_D) | \bar{c} \gamma_\mu b | B(p_B) \rangle \\ = 2f_+^{BD}(q^2)p_\mu + [f_+^{BD}(q^2) + f_-^{BD}(q^2)]q_\mu, \end{aligned} \quad (1)$$

in which $q = (p_B - p_D)$ is the momentum transfer and only the vector current $\bar{c} \gamma_\mu b$ contributes to the pseudoscalar-to-pseudoscalar amplitude for the non-perturbative matrix elements $\langle D(p) | \bar{c} \gamma_\mu b | B(p_B) \rangle$. Meanwhile, it also can be expressed in the following form:

$$\begin{aligned} \langle D(p_D) | \bar{c} \gamma_\mu b | B(p_B) \rangle = \sqrt{m_B m_D} [h_+(w)(v_B + v_D)_\mu \\ + h_-(w)(v_B - v_D)_\mu], \end{aligned} \quad (2)$$

where the functions $h_+(w)$ and $h_-(w)$ are a combination of the $B \rightarrow D$ TFF $\mathcal{G}(w)$, *i.e.*,

$$\mathcal{G}(w) = h_+(w) - \frac{m_B - m_D}{m_B + m_D} h_-(w). \quad (3)$$

Moreover, the relation between the two $B \rightarrow D$ TFFs $\mathcal{G}(w)$ and $f_+^{BD}(q^2)$, is given by

$$f_+^{BD}(q^2) = \frac{m_B + m_D}{2\sqrt{m_B m_D}} \mathcal{G}(w) \quad (4)$$

On one hand, BABAR collaboration [8] and Belle collaboration [10, 11] have presented plentiful datasets for the $B \rightarrow D$ vector TFF $\mathcal{G}(w)$ which are shown in Fig. 1. In order to use these information effectively, one can take the MC approach which should proceed from a model-independent formula, based solely on QCD dispersion relations as proposed by Boyd, Grinstein and Lebed

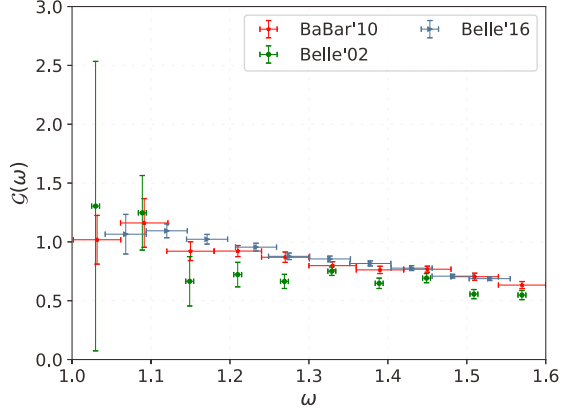


FIG. 1. The experimental data of TFF $\mathcal{G}(w)$ from BABAR'10 [8] and Belle'02 [10] and Belle'16 [11], respectively.

(BGL) [48].

$$f_i(z) = \frac{1}{P_i(z)\phi_i(z)} \sum_{n=0}^N a_{i,n} z^n, \quad i = (+, 0), \quad (5)$$

The letter z is a function of the recoil variable w , which is defined as:

$$z(w) = \frac{\sqrt{w+1} - \sqrt{2}}{\sqrt{w+1} + \sqrt{2}} \quad (6)$$

where w describes the kinematics of the semileptonic decay $B \rightarrow D\ell\nu_\ell$ and represents the product of the four-velocities of the B and D mesons, namely $w = v_B \cdot v_D$ with $v_B = p_B/m_B$ and $v_D = p_D/m_D$. Moreover, the $P_i(z)$ are the ‘‘Blaschke factors’’ that incorporates the apparent pole in q^2 and one can choose $P_i(z) = 1$ as stated in Ref. [24]. The $a_{i,n}$ are free parameters, and index n denotes the order at which the sequence is truncated. $\phi_i(z)$ represent the ‘‘outer functions’’, which are arbitrary but must be analytic, with no poles or branch cuts and

$$\begin{aligned} \phi_+(z) &= 1.1213(1+z)^2(1-z)^{\frac{1}{2}} \\ &\quad \times [(1+r)(1-z) + 2\sqrt{r}(1+z)]^{-5}, \quad (7) \end{aligned}$$

$$\begin{aligned} \phi_0(z) &= 0.5299(1+z)(1-z)^{3/2} \\ &\quad \times [(1+r)(1-r) + 2\sqrt{r}(1+z)]^{-4}, \quad (8) \end{aligned}$$

Where $r = m_D/m_B$. With the choice of the outer function, the coefficients $a_{i,n}$ possess a relatively simple form of uniformity. The coefficient $a_{i,n}$ in Eq. (5) satisfies the condition of uniformity $\sum_{n=0}^N |a_{i,n}|^2 \leq 1$ for any order n . At this stage, the formulaic requirements for performing the MC fitting of $B \rightarrow D$ TFF $\mathcal{G}(w)$ are sufficient.

On the other hand, one can choose the following two-point correlation function from the vacuum to the meson to obtain the improved LCSRs analytical expression of the $B \rightarrow D$ vector TFF $f_+^{BD}(q^2)$:

$$\Pi_\mu(p, q) = i \int d^4x e^{ipx} \langle D(p) | T \{ \bar{c}(x) \gamma_\mu (1 + \gamma_5) b(x) \} | 0 \rangle$$

$$\begin{aligned} &\times \bar{b}(0) i (1 + \gamma_5) d(0) \rangle | 0 \rangle \\ &= \Pi(q^2, (p+q)^2) p_\mu + \tilde{\Pi}(q^2, (p+q)^2) q_\mu. \quad (9) \end{aligned}$$

Here, we use the right-hand chiral current $\bar{b}(0) i (1 + \gamma_5) d(0)$ instead of traditional current $\bar{b}(0) i \gamma_5 d(0)$, which can suitably eliminate the uncertainty introduced by the twist-3 LCDAs and make twist-2 LCDA dominate contribution [49]. This can effectively make up for our lack of understanding of the twist-3 wave function and the lack of corresponding $\mathcal{O}(\alpha_s)$ correction. Next, one need to do a two-step process with Eq. (9). Firstly, we can insert the complete set of states between the currents in Eq. (9) with the same quantum numbers as $\bar{b}(0) i \gamma_5 d(0)$ in the timelike q^2 -region and isolate the pole term of the lowest pseudoscalar B -meson. Then, a threshold s_0 will be introduced to separate the ground state B and the excited state B^H . In the case of the right-hand chiral current, the B^H will include the scalar resonances. Therefore, the s_0 should be set near the lowest scalar B -meson. After replacing the contributions from the higher resonances and continuum states with dispersion integrations, the hadronic expression can be obtained. Secondly, in the QCD theory, the correlator can be calculated by carrying out the operator product expansion (OPE) near the small light cone distance $x^2 \approx 0$ in the spacelike q^2 -region, where main nonperturbative inputs are parameterized into the LCDAs of the final meson. Then, with the help of the dispersion relation and quark hadron duality, the OPE expansion can be matched with the hadron expression. In order to remove the subtraction term in the dispersion relation and exponentially suppress the contribution of unknown excitation resonance, one needs to use the Borel transformation. Finally, the LCSRs for the TFF $f_+^{BD}(q^2)$ can be obtained

$$\begin{aligned} f_+^{BD}(q^2) &= \frac{m_b^2 f_D}{m_B^2 f_B} e^{\frac{m_B^2}{M^2}} \left\{ \int_{\Delta}^1 du \exp\left[-\frac{m_b^2 - \bar{u}(q^2 - um_D^2)}{uM^2}\right] \right. \\ &\quad \times \left[\frac{\phi_D(u)}{u} - \frac{8m_b^2 [g_1(u) + G_2(u)]}{u^3 M^4} + \frac{2g_2(u)}{uM^2} \right] \\ &\quad + \int_0^1 dv \int D\alpha_i \frac{\theta(\xi - \Delta)}{\xi^2 M^2} \exp\left[-\frac{m_b^2 - \bar{\xi}(q^2 - \xi m_D^2)}{\xi M^2}\right] \\ &\quad \left. \times [2\varphi_\perp(\alpha_i) + 2\tilde{\varphi}_\perp(\alpha_i) - \varphi_\parallel(\alpha_i) - \tilde{\varphi}_\parallel(\alpha_i)] \right\}, \quad (10) \end{aligned}$$

in which $\bar{u} = 1 - u$, $\xi = \alpha_1 + v\alpha_3$, $\bar{\xi} = 1 - \xi$, $G_2(u) = \int_0^u g_2(v) dv$ and the integration upper limit is

$$\begin{aligned} \Delta &= \frac{1}{2m_D^2} \left[\sqrt{(s_0 - q^2 - m_D^2)^2 + 4m_D^2(m_b^2 - q^2)} \right. \\ &\quad \left. - (s_0 - q^2 - m_D^2) \right], \quad (11) \end{aligned}$$

where s_0 is the continuum threshold. Furthermore, the functions $g_1(u)$, $g_2(u)$, $\varphi_{\perp(\parallel)}(\alpha_i)$, $\tilde{\varphi}_{\perp(\parallel)}(\alpha_i)$ are the two-particle and three-particle twist-4 LCDAs, respectively, which are similar to the kaonic case with $SU_f(3)$ -breaking

effect, as introduced in Ref. [50]. When the masses of the quarks are considered to be infinitely large, our current TFF $f_+^{BD}(q^2)$ aligns with the Isgur-Wise function for TFFs between heavy mesons, as reported in Refs. [51, 52]. This indicates that, at least at the leading order, LCSRs for $f_+^{BD}(q^2)$ are equivalent to estimates derived from heavy quark symmetry. However, at the next-to-leading order (NLO) level, the influence of heavy quark masses may introduce discrepancies between these two approaches, which is beyond the scope of this paper. For ease of comparison with experimental analyses found in the literature, we also provide LCSRs for the $B \rightarrow D$ TFF within the framework of heavy quark symmetry.

For the D -meson leading-twist LCDA $\phi_{2;D}(x, \mu_0^2)$, it accounts for the dominant contribution to the $B \rightarrow D$ TFF due to the chiral correlation function (9). Therefore, to obtain an accurate behavior of the D -meson leading-twist LCDA, a new LCDA is constructed using the light-cone harmonic oscillator (LCHO) model, which has been successfully applied to pseudoscalar mesons π, K [53–56], scalar mesons $a_0(980), K_0^*(1430)$ [57–60], and vector mesons ρ, ϕ [61, 62], etc. Generally, the D -meson leading-twist LCDA $\phi_{2;D}(x, \mu_0^2)$ and its wave function (WF) $\psi_{2;D}(x, \mathbf{k}_\perp)$ have the definition as follows:

$$\phi_{2;D}(x, \mu_0^2) = \frac{2\sqrt{6}}{f_D} \int_{|\mathbf{k}_\perp|^2 \leq \mu_0^2} \frac{d\mathbf{k}_\perp}{16\pi^3} \psi_{2;D}(x, \mathbf{k}_\perp), \quad (12)$$

where f_D is decay constant and \mathbf{k}_\perp stands for the transverse momentum. For the WF $\psi_{2;D}(x, \mathbf{k}_\perp)$, one can establish a relation between the equal-time WF in the rest frame and light cone WF in the finite momentum frame based on the Brodsky-Huang-Lepage (BHL) description, which can be written as

$$\psi_{2;D}(x, \mathbf{k}_\perp) = \chi_{2;D}(x, \mathbf{k}_\perp) \psi_{2;D}^R(x, \mathbf{k}_\perp), \quad (13)$$

where the total spin-space WF is

$$\chi_{2;D}(x, \mathbf{k}_\perp) = \frac{\bar{x}m_c + xm_d}{\sqrt{\mathbf{k}_\perp^2 + (\bar{x}m_c + xm_d)^2}}, \quad (14)$$

while the spital WF can be expressed as,

$$\psi_{2;D}^R(x, \mathbf{k}_\perp) = A_{2;D} [1 + B_{2;D} C_2^{3/2}(x - \bar{x})] \times \exp \left[-b_{2;D}^2 \left(\frac{\mathbf{k}_\perp^2 + m_c^2}{x} + \frac{\mathbf{k}_\perp^2 + m_c^2}{\bar{x}} \right) \right]. \quad (15)$$

After integrating over the transverse momentum dependence \mathbf{k}_\perp , one can obtain the D -meson leading-twist LCDA $\phi_{2;D}(x, \mu_0^2)$, namely:

$$\begin{aligned} \phi_{2;D}(x, \mu_0^2) &= \frac{A_{2;D} \sqrt{6x\bar{x}Y}}{8\pi^{3/2} f_D b_{2;D}} [1 + B_{2;D} \times C_2^{3/2}(x - \bar{x})] \\ &\times \exp \left[-b_{2;D}^2 \frac{xm_d^2 + \bar{x}m_c^2 - Y^2}{x\bar{x}} \right] \\ &\times \left[\text{Erf} \left(\frac{b_{2;D} \sqrt{\mu_0^2 + Y^2}}{\sqrt{x\bar{x}}} \right) - \text{Erf} \left(\frac{b_{2;D} Y}{\sqrt{x\bar{x}}} \right) \right], \quad (16) \end{aligned}$$

where $A_{2;D}$ is the normalization, and $b_{2;D}$ is harmonious parameters dominates the WF's transverse distribution. The $B_{2;D}$ is free parameter, which will be discussed in the following section. The error function $\text{Erf}(x)$ is defined as $\text{Erf}(x) = 2 \int_0^x \exp(-t^2) dt / \sqrt{\pi}$, $Y = xm_d + \bar{x}m_c$ and $\bar{x} = (1 - x)$. Additionally, the parameters $A_{2;D}$ and $b_{2;D}$ can be further constrained in terms of the following formulas:

- The WF normalization condition:

$$\int_0^1 dx \int \frac{d^2\mathbf{k}_\perp}{16\pi^3} \psi_{2;D}(x, \mathbf{k}_\perp) = \frac{f_D}{2\sqrt{6}}. \quad (17)$$

- The probability of finding the leading valence-quark state in D -meson (P_D), which is $\simeq 0.8$ [63–65], as defined in the following form:

$$P_D = \int_0^1 dx \int_{|\mathbf{k}_\perp|^2 \leq \mu_0^2} \frac{d^2\mathbf{k}_\perp}{16\pi^3} |\psi_{2;D}(x, \mathbf{k}_\perp)|^2. \quad (18)$$

Once the free parameter $B_{2;D}$ is established, the remaining input parameters can be calculated using the aforementioned two formulas, ultimately allowing for the determination of the specific characteristics of the WF/LCDA.

Finally, to calculate the corresponding decay branching ratio, the following formula can be used to define the decay width of the semileptonic decay $B \rightarrow D$ correlation

$$\begin{aligned} \frac{d\Gamma}{dq^2}(B \rightarrow D \ell \bar{\nu}_\ell) &= \frac{G_F^2 |V_{cb}|^2}{192\pi^3 m_B^3} \left(1 - \frac{m_\ell^2}{q^2} \right)^2 \\ &\times \left[\left(1 + \frac{m_\ell^2}{2q^2} \right) \lambda^{\frac{3}{2}}(q^2) |f_+^{BD}(q^2)|^2 \right. \\ &\left. + \frac{3m_\ell^2}{2q^2} (m_B^2 - m_D^2)^2 \lambda^{\frac{1}{2}}(q^2) |f_0^{BD}(q^2)|^2 \right], \quad (19) \end{aligned}$$

Here, the Fermi constant $G_F = 1.166 \times 10^{-5} \text{ GeV}^{-2}$, and the phase space factor $\lambda(q^2) = (m_B^2 + m_D^2 - q^2)^2 - 4m_B^2 m_D^2$. When the lepton mass m_ℓ is ignored, *i.e.*, $m_\ell \rightarrow 0$, the decay width will only have the contribution from the vector TFF $f_+^{BD}(q^2)$.

III. NUMERICAL RESULTS AND DISCUSSIONS

In order to carry out the phenomenological analysis, the following input parameters are adopted: for the b, c -quark masses, we take $m_b = 4.85 \pm 0.05 \text{ GeV}$ and $m_c = 1.5 \pm 0.05 \text{ GeV}$, while the masses of B -meson and D -meson are $m_B = 5.279 \text{ GeV}$ and $m_D = 1.869 \text{ GeV}$, as listed by the Particle Data Group (PDG) [66]. For the decay constants of B -meson and D -meson, we take $f_B = 0.207_{-0.009}^{+0.017}$ and $f_D = 0.201_{-0.013}^{+0.012}$ [67]. By extracting the data points of TFF from the BABAR and Belle Collaborations, we employ the MC method for fitting

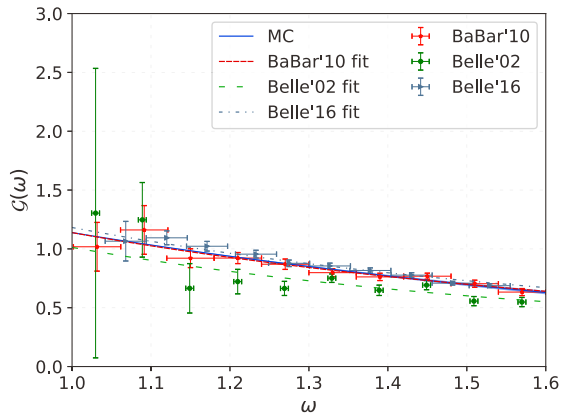


FIG. 2. Under the MC method, the fitting results are derived separately from the experimental data of *BABAR*'10 [8], Belle'02 [10], and Belle'16 [11], as well as from a comprehensive consideration of all data points.

and ensure they are reasonably dispersed throughout the study area, as shown in Fig. 2. The fitting result not only improves the accuracy but also reflects a more comprehensive connection between $\mathcal{G}(\omega)$ and ω . The description in Fig. 2 is described in detail below.

- In Fig. 2, the extracted $B \rightarrow D$ TFF data sets from the *BABAR* [8] and Belle [10, 11] Collaborations are shown, respectively. The red dashed lines, green dashed-dotted lines, and gray dashed lines represent the fitted results for each experiment data set, obtained using the MC method. Moreover, the solid line stands for the total fitted results of three experimental data sets. This result is obtained by taking into account the central values and uncertainties of the three experimental data sets, comprehensively.
- By examining the lines in Fig. 2, the total fitted result exhibits better behavior compared to other three fitted curves, which may enable more accurate theoretical predictions for the physical observables of the semileptonic decays $B \rightarrow D\ell\bar{\nu}_\ell$.

To validate the reliability of the results derived from the MC method, the average acceptance rate (AAR) outcomes obtained through fitting are presented in Table I. The average acceptance rate serves as a crucial metric for evaluating the quality of the fit, with the generally accepted range being [0.2, 0.5] [68]. Notably, the fitting results of the three experiments all fall within this range. By comprehensively considering all the shape factor data points, we obtain a curve with an average acceptance rate of 0.235, which is remarkably close to the optimal average acceptance rate of 0.234 reported in Ref. [69]. Consequently, this indicates that the results obtained via this method possess a high degree of credibility.

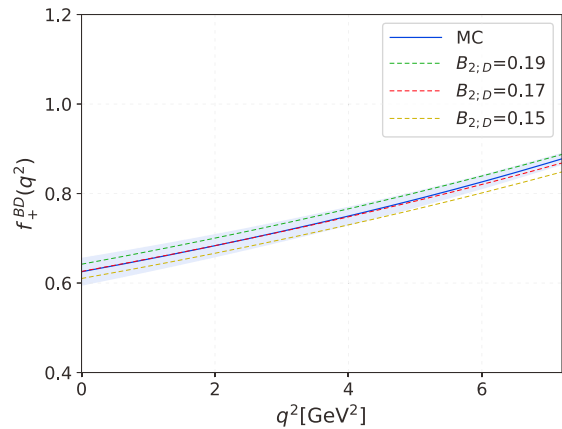


FIG. 3. The TFFs $f_+^{BD}(q^2)$ versus q^2 . The solid line is the MC fit and the shadow bands represent errors. The dashed lines represent the central results of LCSR under different LCDA parameters, respectively.

Next, for the $B \rightarrow D$ TFF calculated by LCSRs, the non-perturbative input parameter twist-2 LCDA $\phi_{2;D}(x, \mu_0^2)$ needs to be determined, but there remains an undetermined free parameters $B_{2;D}$. Therefore, to achieve better performance, we need to use the MC-fitted $f_+^{BD}(q^2)$ result obtained with the help of Eq. (4) as a reference for the determination. After $B_{2;D}$ is determined, other parameters $A_{2;D}$ and $b_{2;D}$ can be determined by two constraint conditions, *i.e.*, the normalization condition, and the probability of the leading valence-quark state in D -meson, which is $P_D \simeq 0.8$ [63–65]. These constraints serve as additional theoretical restrictions, enabling us to determine the behavior of the LCDA more precisely, thereby facilitating a more profound understanding and analysis of $\phi_{2;D}(x, \mu_0^2)$. In addition, we need to determine both the continuum threshold s_0 and Borel parameter M^2 simultaneously. The following criteria can be used:

- To determine the value of M^2 , we require that the contribution of the continuous states is less than 30% of the total LCSRs;
- It is also required that the contribution of twist-4 LCDAs does not exceed 5%, Therefore, the contribution of twist-4 is neglected;
- Within the Borel window, the changes of TFFs does not exceed 10%;
- The continuum threshold s_0 , serving as the boundary between the ground state contributions and higher-mass contributions of B -meson, is generally set close to the square of the mass of the first excited state of B -meson.

After followed by the above criteria, we determined the continuum threshold $s_0 = 39(2) \text{ GeV}^2$ and Borel win-

TABLE I. Fitted parameters and average acceptance rate (AAR)

	MC	BABAR'10	Belle'02	Belle'16
a_0	0.0120	0.0120	$0.0106^{+0.0001}_{-0.0001}$	$0.0124^{+0.00005}_{-0.00005}$
a_1	$-0.0715^{+0.0013}_{-0.0013}$	$-0.0795^{+0.0015}_{-0.0015}$	$-0.0806^{+0.0037}_{-0.0037}$	$-0.0834^{+0.0028}_{-0.0028}$
a_2	$0.0288^{+0.0223}_{-0.0223}$	$0.1796^{+0.0284}_{-0.0284}$	$0.2600^{+0.0382}_{-0.0382}$	$0.2170^{+0.0355}_{-0.0355}$
AAR	0.235	0.270	0.425	0.378

TABLE II. The D -meson leading-twist LCDAs $\phi_{2,D}(x, \mu_0^2)$ for typical $B_{2,D}$ within the region of $[0.15, 0.19]$, at $\mu_0 = 2$ GeV.

$B_{2,D}$	$A_{2,D}$	$b_{2,D}$
0.15	293.1	0.720
0.17	288.4	0.718
0.19	283.7	0.716

dow is taken as $M^2 = 17(2)$ GeV². In order to graphically show that after determining these important input parameters, the results of LCSRs will be highly consistent with the results of MC fitting, we show the $f_+^{BD}(q^2)$ obtained under the two methods in Fig. 3. During this process, the solid line depicts the result obtained through MC fitting, whereas the shaded band distinctly delineates the corresponding uncertainty range, offering an intuitive visual representation for the reader. It is noteworthy that the results of LCSRs are denoted by dotted lines, facilitating comparison with our calculations to ascertain the consistency and applicability of the model. Since the LCSRs method is only effective in the lower and intermediate q^2 regions, in Fig. 3, we only show the behavior of the TFF obtained from MC fitting and LCSRs in the $0 \leq q^2 \leq 7.2$ GeV² region. We can clearly see that in this region, our results are highly consistent with the results of MC fitting, which ensures the rationality of our determination of unknown parameters. More specifically, we set an appropriate range for the free parameter $B_{2,D}$, then determine another two parameters $A_{2,D}, b_{2,D}$ based on the constraint conditions. This allow us to obtain the behavior of D -meson twist-2 LCDA, which is then used to calculate the corresponding $B \rightarrow D$ TFF. Finally, the fitted TFF is matched to yield the final LCSRs TFF.

Furthermore, through careful comparison and analysis, we successfully determine that the reasonable range for the free parameter

$$B_{2,D} = 0.17 \pm 0.02. \quad (20)$$

The corresponding values of $A_{2,D}$ and $b_{2,D}$ are listed in Table II. To visually and intuitively demonstrate the specific behavior of the D -meson leading-twist LCDA $\phi_{2,D}(x, \mu_0^2)$, we plot it under different models in Fig. 4. And other prediction from the KLS model [15], LLZ model [70], LM model [71], LFQM model [72], and LCHO

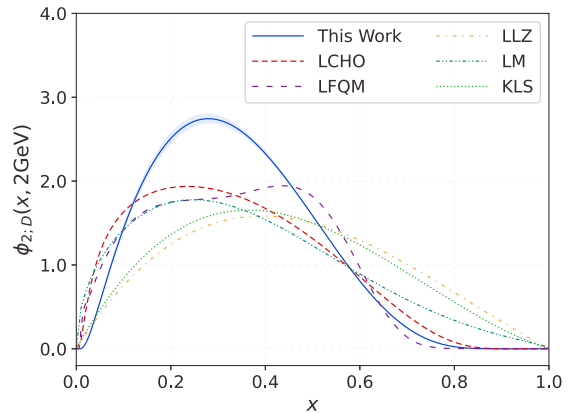


FIG. 4. Curves of the D -meson leading-twist LCDA $\phi_{2,D}(x, \mu_0^2)$ at scale $\mu_0 = 2$ GeV. The LCDA models in literatures such as KLS model [15], LLZ model [70], LM model [71], the form with LFQM [72], and LCHO model [73] are also shown for comparison.

model [73] are also shown for comparison. The detailed descriptions are listed as follows.

- In Fig. 4, the solid line represents our model and the shadow band represents the error range caused by the input parameters $B_{2,D}, A_{2,D}$ and $b_{2,D}$. While the blue dashed line, cyan dashed line, orange dashed line, red dashed line, and purple dashed line, respectively, represent the LFQM model, KLS model, LLZ model, LM model, and LCHO model;
- As illustrated in Fig. 4, it is evident that the tendencies of all the models display a certain degree of consistency. Nevertheless, our $\phi_{2,D}(x, \mu_0^2)$ model exhibits a more restricted behavior specifically within the low x -region. It possesses a peak within the range of x approximately between 0.2 and 0.3, which is in alignment with the LM and LCHO models; yet, it diverges from the KLS, LLZ, and LFQM models. The latter models, in contrast, reach a peak at a relatively larger x value, approximately within the range of 0.3 to 0.5.

In order to access the information of $B \rightarrow D$ TFF in the whole kinematic region, we need to extrapolate the LCSRs predictions obtained above toward large

TABLE III. TFFs of the $B \rightarrow D$ transition at large recoil point. As a comparison, we also present other predictions.

	$f_+^{BD}(0)$
LCSR (This Work)	$0.625^{+0.087}_{-0.113}$
MC (This Work)	0.625 ± 0.031
pQCD'13 [13]	$0.520^{+0.12}_{-0.10}$
LCSR'14 [18]	$0.653^{+0.004}_{-0.011}$
LCSR'17 [19]	$0.673^{+0.038}_{-0.041}$
LCSR'22 [21]	0.552 ± 0.216
LCSR'18 [22]	$0.659^{+0.029}_{-0.032}$
LQCD'19 [23]	0.658 ± 0.017
FNAL/MILC'15 [24]	0.672 ± 0.027
HPQCD'16 [29]	0.664 ± 0.034

momentum transfer with a certain parametrization for TFFs. The physically allowable ranges for the TFFs are $0 \leq q^2 \leq q_{\max}^2 = (m_B - m_D)^2 \sim 11.6 \text{ GeV}^2$. One can extrapolate it to whole q^2 -regions via a rapidly $z(q^2, t)$ converging the simplified series expansion (SSE), *i.e.*, the TFFs are expanded as [74, 75]:

$$f_+^{BD}(q^2) = \frac{1}{1 - q^2/m_{B^2}} \sum_{k=0,1,2} \beta_k z^k(q^2, t_0) \quad (21)$$

where β_k are real coefficients and $z(q^2, t)$ is the function,

$$z^k(q^2, t_0) = \frac{\sqrt{t_+ - q^2} - \sqrt{t_+ - t_0}}{\sqrt{t_+ - q^2} + \sqrt{t_+ - t_0}}, \quad (22)$$

with $t_{\pm} = (m_B \pm m_D)^2$ and the auxiliary parameter $t_0 = t_{\pm}(1 - \sqrt{1 - t_-/t_+})$. The SSE method possesses superior merit, which keeps the analytic structure correct in the complex plane and ensures the appropriate scaling, $f_+^{BD}(q^2) \sim 1/q^2$ at large q^2 . And the quality of fit Δ is devoted to take stock of the result of extrapolation, which is defined as

$$\Delta = \frac{\sum_t |F_i(t) - F_i^{\text{fit}}(t)|}{\sum_t |F_i(t)|} \times 100. \quad (23)$$

After making an extrapolation for the TFFs $f_+^{BD}(q^2)$ to the whole physical q^2 -region. Then, the behaviors of $B \rightarrow D$ TFFs in the whole physical region with respect to squared momentum transfer are given in Fig. 5. Then, we also calculate the numerical result of the $B \rightarrow D\ell\bar{\nu}_\ell$ TFF $f_+^{BD}(q^2)$ at the large recoil region and give its numerical result in Table III as well as the comparison with other theoretical and experimental groups, which will be described in detail below.

- In Fig. 5, the darker band represents the LCSR result of our prediction, while the lighter band represents the SSE prediction;
- In Fig. 5, we exhibit the theoretical predictions and experimental results for comparison, such

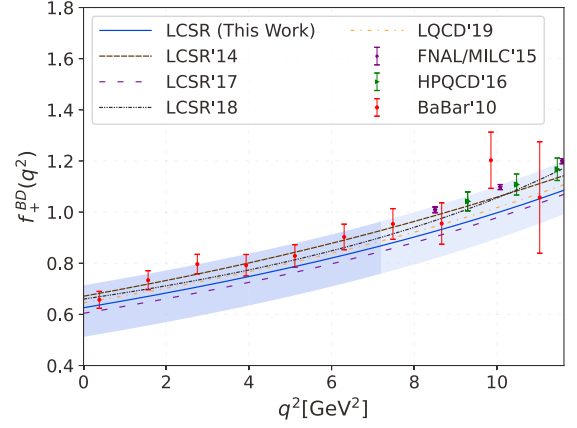


FIG. 5. The TFFs $f_+^{BD}(q^2)$ versus q^2 . The solid line depicts the work, while the shaded area denotes the error. The dotted lines in brown, purple, black, and yellow represent LCSR'14 [18], LCSR'17 [19], LCSR'18 [22], and LQCD'19 [23], respectively. The Red, purple, and green error bars represent the results predicted by BABAR'10 [8], FNAL/MILC'15 [24] and HPQCD'16 [29], respectively.

as LCSR'14(17,18) [18, 19, 22], LQCD'19 [23], FNAL/MILC'15 [24], and HPQCD'16 [29]. Upon comparison, it is evident that our results and their associated uncertainties exhibit strong agreement with those from other predictions, thereby reinforcing the applicability of our D -meson twist-2 LCDA model.

- In Table III, we present the predictions for the $B \rightarrow D$ TFF $f_+^{BD}(0)$ at large recoil region, alongside other results for comparison. Upon comparison, we find that our results are consistent with those of other theoretical and experimental groups, falling within the margin of error.

Furthermore, we will discuss the alternative form for the $B \rightarrow D$ TFF, namely $\mathcal{G}(\omega)$. In relevant research, $\mathcal{G}(\omega)$ is extensively applied within the theoretical framework of pQCD and in the analysis of experimental data. Particularly, the precise determination of $\mathcal{G}(\omega)$ is crucial for accurately extracting the CKM matrix element $|V_{cb}|$ [7]. The CKM matrix elements are fundamental parameters that describe the mixing and decay of different quark flavors, and the precise determination of these elements is crucial for understanding the SM and its extensions. Experimentally, $\mathcal{G}(\omega)$ is usually parameterized as the following expansion:

$$\mathcal{G}_D(\omega) = \mathcal{G}_D(1) \left[1 - \hat{\rho}_D^2(\omega - 1) + \hat{c}_D(\omega - 1)^2 + \mathcal{O}((\omega - 1)^3) \right]. \quad (24)$$

For comparison with our theoretical estimate, we also include the results from the parameterization formula (24). In Fig. 6, the solid blue line represents the

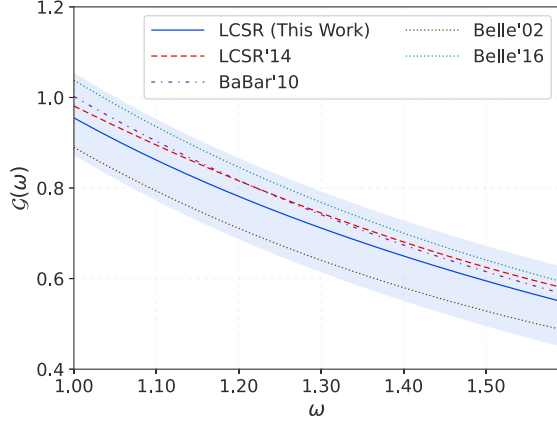


FIG. 6. The TFFs $\mathcal{G}(\omega)$ versus ω . The solid blue line represents the LCSR prediction, and the shaded area represents its error. Solid red lines, dashed purple lines, dashed brown lines, and dashed cyan lines represent the predictions of LCSR'14 [18], BABAR'10 [8], Belle'02 [10], and Belle'16 [11], respectively.

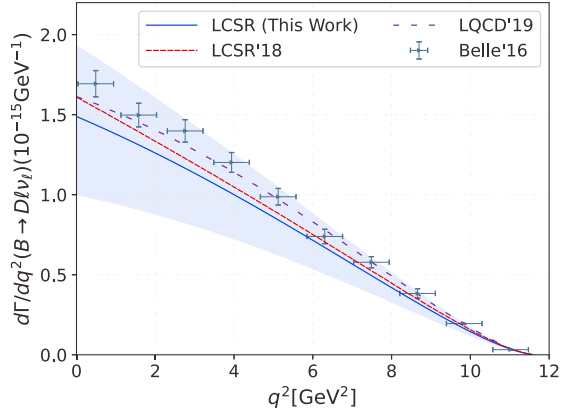


FIG. 7. The differential decay width for $B \rightarrow D\ell\nu_\ell$ within uncertainties (in unit: 10^{-15}). The solid blue line is the result of our central value and shaded area represents the error. As a comparison, we also give a prediction of the cooperation between LQCD'19 [23], LCSR'18 [22] and Belle'16 [11].

MC prediction, with the shaded blue area indicating its error. The dashed purple line represents the LCSRs prediction, and the lightly shaded area represents its error. The dashed red, purple, brown, and cyan lines represent the predictions of LCSR'14 [18], BABAR'10 [8], and Belle'02 [10], and Belle'16 Collaborations [11], respectively. As shown in the Fig. 6, our predictions for $\mathcal{G}(\omega)$ using both the LCSRs and MC methods are in good agreement with the data.

At this stage, we begin to compute the branching ratios of the semileptonic decays $B \rightarrow D\ell\nu_\ell$ in terms of the $B \rightarrow D$ TFF obtained from both the LCSRs and MC approaches. The CKM matrix elements $|V_{cb}|$ is a cru-

TABLE IV. The branching ratio results for $B^0 \rightarrow D^-\ell^+\nu_\ell$ and $B^+ \rightarrow \bar{D}^0\ell^+\nu_\ell$ are presented here. At the same time, other experimental and theoretical results are used for comparison.

	Decay Channel	Branching ratios
LCSR (This Work)	$B^0 \rightarrow D^-\ell^+\nu_\ell$	$(1.96^{+0.51}_{-0.55})\%$
	$B^+ \rightarrow \bar{D}^0\ell^+\nu_\ell$	$(2.12^{+0.55}_{-0.59})\%$
MC (This Work)	$B^0 \rightarrow D^-\ell^+\nu_\ell$	$(1.97^{+0.128}_{-0.123})\%$
	$B^+ \rightarrow \bar{D}^0\ell^+\nu_\ell$	$(2.13^{+0.137}_{-0.132})\%$
CLEO'19 [6]	$\bar{B}^0 \rightarrow D^+\ell^-\bar{\nu}$	$(1.87 \pm 0.15 \pm 0.32)\%$
	$B^- \rightarrow D^0\ell^-\bar{\nu}$	$(1.94 \pm 0.15 \pm 0.34)\%$
BABAR'10 [8]	$\bar{B}^0 \rightarrow D^+\ell^-\bar{\nu}$	$(2.23 \pm 0.11 \pm 0.11)\%$
	$B^- \rightarrow D^0\ell^-\bar{\nu}$	$(2.31 \pm 0.08 \pm 0.09)\%$
BABAR'23 [9]	$\bar{B} \rightarrow D\ell^+\bar{\nu}_\ell$	$(2.15 \pm 0.11 \pm 0.14)\%$
Belle'16 [11]	$\bar{B}^0 \rightarrow D^+\ell^-\bar{\nu}$	$(2.31 \pm 0.03 \pm 0.11)\%$
Belle-II'22 [12]	$B^0 \rightarrow D^-e^+\nu_e$	$(1.99 \pm 0.04 \pm 0.08)\%$
	$B^+ \rightarrow \bar{D}^0e^+\nu_e$	$(2.21 \pm 0.03 \pm 0.08)\%$
pQCD'13 [13]	$\bar{B}^0 \rightarrow D^+\ell^-\bar{\nu}_\ell$	$(2.03^{+0.92}_{-0.70})\%$
LCSR'14 [18]	$B^0 \rightarrow D^-\ell^+\nu_\ell$	$(2.18 \pm 0.12)\%$
	$B^+ \rightarrow \bar{D}^0\ell^+\nu_\ell$	$(2.26 \pm 0.11)\%$
LCSR'17 [19]	$\bar{B}^0 \rightarrow D^+\ell\nu_\ell$	$(2.132 \pm 0.273)\%$

cial input parameter in computation, which is taken as $|V_{cb}| = (41.09 \pm 1.16) \times 10^{-3}$ [9]. After considering the B -meson lifetime τ_B , the numerical results of $\mathcal{B}(B \rightarrow D\ell\nu_\ell)$ are presented in Table IV. We also plot the differential decay width of the semileptonic decays $B \rightarrow D\ell\nu_\ell$ in Fig. 7, where other theoretical and experimental results are shown for comparison, such as the Belle'16 Collaboration [11], LCSR'18 [22], and LQCD'19 [23]. Furthermore, we also compare our results with those from theoretical predictions and experimental observations to assess their consistency in Table IV. The table includes results from the theoretical groups pQCD'13 [13], LCSR'14 [18], LCSR'17 [19], as well as from experimental groups Belle-II'16 [11], Belle-II'22 [12], BABAR'23 [9], BABAR'10 [8] and CLEO'19 [6]. Our comparison reveals certain deviations from the results of other groups, which may primarily stem from uncertainties in the input parameters. However, within the estimated error range, these results remain reasonable.

In addition, in order to provide a new result about $|V_{cb}|$ in the QCD LCSRs and the MC methods, we extract the CKM matrix element $|V_{cb}|$ based on the branching ratio $B^+ \rightarrow \bar{D}^0\ell^+\nu_\ell$ and $B^0 \rightarrow D^-\ell^+\nu_\ell$ in BABAR'23 [9] and Belle'22 [12], respectively. The result is as follows:

$$|V_{cb}|_{\text{SR}} (B^+\text{-Channel}) = 41.93^{+1.03}_{-1.05} \times 10^{-3} \quad (25)$$

$$|V_{cb}|_{\text{MC}} (B^+\text{-Channel}) = 41.82^{+0.23}_{-0.25} \times 10^{-3} \quad (26)$$

$$|V_{cb}|_{\text{SR}} (B^0\text{-Channel}) = 42.97^{+2.42}_{-2.57} \times 10^{-3} \quad (27)$$

$$|V_{cb}|_{\text{MC}} (B^0\text{-Channel}) = 42.82^{+1.07}_{-1.29} \times 10^{-3} \quad (28)$$

For comparison, we have collected the results of the

TABLE V. Our prediction of $|V_{cb}|$ obtained from the decay channels $B^+ \rightarrow \bar{D}^0 \ell^+ \nu_\ell$ and $B^0 \rightarrow D^- \ell^+ \nu_\ell$, compared with other theoretical and experimental results of various channels (in unit 10^{-3}).

$ V_{cb} $	B^+ -Channel	B^0 -Channel
LCSR (This Work)	$41.93^{+1.03}_{-1.05}$	$42.97^{+2.42}_{-2.57}$
MC (This Work)	$41.82^{+0.23}_{-0.25}$	$42.82^{+1.07}_{-1.29}$
PDG [66]	41.1 ± 1.2	41.1 ± 1.2
BABAR'10 [8]	38.47 ± 0.90	38.22 ± 0.90
BABAR'23 [9]	41.09 ± 1.16	/
Belle'16 [11]	40.83 ± 1.13	40.83 ± 1.13
Belle'22 [12]	38.28 ± 1.16	38.28 ± 1.16
LCSR'14 [18]	$41.28^{+5.68}_{-4.82}$	$40.44^{+5.56}_{-4.72}$
LCSR-II'22 [21]	$40.2^{+0.6}_{-0.5}$	$40.9^{+0.6}_{-0.5}$
LQCD'19 [23]	41.01 ± 0.75	/
FNAL/MILC'15 [24]	$39.6 \pm 1.7 \pm 0.2$	/
HPQCD'16 [29]	/	$40.2 \pm 0.017 \pm 0.013$

CKM matrix element $|V_{cb}|$ from both theoretical and experimental studies. The results are presented in Table V, where it can be seen that our predictions for the CKM matrix element $|V_{cb}|$ agree well with other theoretical and experimental results.

IV. SUMMARY

In this paper, we utilize the MC method in combination with the LCSRs method to investigate the key component of $B \rightarrow D$ semileptonic decay, specifically the $B \rightarrow D$ TFFs. Firstly, the experimental data points for TFF $\mathcal{G}(w)$ both from BABAR and Belle Collaborations were collected. We give the TFF $\mathcal{G}(w)$ behaviors obtained from simulating these data points using the MC method for three separate experiments. After considering all the data points comprehensively, we fitted one curve that serves as the main reference in this paper. To demonstrate the credibility of the results obtained using this method, we present the relevant fitting parameters and the key indicator for assessing the goodness of fit, namely the average acceptance rate in Table I. Among them, considering all data points, the average acceptance rate of the MC is in high agreement with the optimal value.

Then we calculate the $B \rightarrow D$ vector TFF $f_+^{BD}(q^2)$ by using the LCSRs approach. The vector TFF from MC method are taken as criterion. When taking the undetermined free parameter $B_{2;D} = 0.17 \pm 0.02$ through comparison, we get the two curves of vector TFF that overlap with each other. In Fig. 3, we present a comparison between LCSRs and MC in the lower and intermediate q^2 region. The high degree of overlap between the two curves indicates the good accuracy of our parameters. Furthermore, we have listed the $f_+^{BD}(q^2)$ at large recoil region obtained by using the LCSRs method in comparison with other theoretical predictions. The specific numerical values have been listed in Table II, and we have presented the behavioral trend of the $\phi_{2;D}(x, \mu_0^2)$ in Fig. 4, which also includes predictions from KLS model, LLZ model, LM model, LFQM model, and LCHO model. Meanwhile, we utilize the criteria of LCSRs to ascertain the continuum threshold s_0 and Borel parameter M^2 . Subsequently, the $f_+^{BD}(q^2)$ is extrapolated to the entire q^2 region using the SSE method, and compared with other theoretical and experimental predictions in the Fig. 5. The behavior of another form of TFF $\mathcal{G}(w)$ is also presented.

Finally, we calculate the differential and total decay width, branching fractions for semileptonic decay $B^+ \rightarrow \bar{D}^0 \ell^+ \nu_\ell$, $B^0 \rightarrow D^- \ell^+ \nu_\ell$. The values are given in Table. IV, which also include the numerical results from theoretical groups such as LCSRs, PQCD, as well as experimental groups like BABAR, Belle and CLEO Collaborations. Our predicted branching ratio are consistent with the experimental data within errors. And then, we predict the CKM matrix element $|V_{cb}|$ and presented it in Table V. Upon comparison and analysis, it was found to be highly consistent with both theoretical and experimental predictions.

V. ACKNOWLEDGMENTS

Hai-Bing Fu and Tao Zhong would like to thank the Institute of High Energy Physics of Chinese Academy of Sciences for their warm and kind hospitality. This work was supported in part by the National Natural Science Foundation of China under Grant No.12265010, 12265009, the Project of Guizhou Provincial Department of Science and Technology under Grant No.ZK[2023]024.

-
- | | |
|--|--|
| <p>[1] N. Cabibbo, Unitary Symmetry and Leptonic Decays, <i>Phys. Rev. Lett.</i> 10, 531-533 (1963).</p> <p>[2] M. Kobayashi and T. Maskawa, CP Violation in the Renormalizable Theory of Weak Interaction, <i>Prog. Theor. Phys.</i> 49, 652-657 (1973).</p> <p>[3] M. Beneke and T. Feldmann, Symmetry breaking corrections to heavy to light B meson form-factors at large recoil, <i>Nucl. Phys. B</i> 592, 3-34 (2001). [hep-ph/0008255]</p> | <p>[4] T. Blake, G. Lanfranchi and D. M. Straub, Rare B Decays as Tests of the Standard Model, <i>Prog. Part. Nucl. Phys.</i> 92, 50-91 (2017). [arXiv:1606.00916]</p> <p>[5] R. Watanabe, V_{cb} and New Physics, <i>PoS CKM2021</i>, 060 (2023).</p> <p>[6] M. Athanas <i>et al.</i> [CLEO Collaboration], Measurement of the $\bar{B} \rightarrow D \ell \bar{\nu}$ partial width and form-factor</p> |
|--|--|

- parameters, *Phys. Rev. Lett.* **79**, 2208-2212 (1997). [arXiv:hep-ex/9705019]
- [7] J. E. Bartelt *et al.* [CLEO Collaboration], Measurement of the $B \rightarrow D\ell\nu$ branching fractions and form-factor, *Phys. Rev. Lett.* **82**, 3746 (1999). [arXiv:hep-ex/9811042]
- [8] B. Aubert *et al.* [BABAR Collaboration], Measurement of $|V_{cb}|$ and the Form-Factor Slope in $\bar{B} \rightarrow D\ell^-\bar{\nu}_\ell$ Decays in Events Tagged by a Fully Reconstructed B Meson, *Phys. Rev. Lett.* **104**, 011802 (2010). [arXiv:0904.4063]
- [9] J. P. Lees *et al.* [BABAR Collaboration], Model-independent extraction of form factors and $|V_{cb}|$ in $\bar{B} \rightarrow D\ell^-\bar{\nu}_\ell$ with hadronic tagging at BABAR, *Phys. Rev. D* **110**, 032018 (2024). [arXiv:2311.15071]
- [10] K. Abe *et al.* [Belle Collaboration], Measurement of $\mathcal{B}(\bar{B}^0 \rightarrow D^+\ell^-\bar{\nu})$ and determination of V_{cb} , *Phys. Lett. B* **526**, 258-268 (2002). [arXiv:hep-ex/0111082]
- [11] R. Glattauer *et al.* [Belle Collaboration], Measurement of the decay $B \rightarrow D\ell\nu_\ell$ in fully reconstructed events and determination of the Cabibbo-Kobayashi-Maskawa matrix element $|V_{cb}|$, *Phys. Rev. D* **93**, 032006 (2016). [arXiv:1510.03657]
- [12] F. Abudinén *et al.* [Belle-II Collaboration], Determination of $|V_{cb}|$ from $B \rightarrow D\ell\nu$ decays using 2019-2021 Belle II data. [arXiv:2210.13143]
- [13] Y. Y. Fan, W. F. Wang, S. Cheng and Z. J. Xiao, Semileptonic decays $B \rightarrow D^{(*)}\ell\nu$ in the perturbative QCD factorization approach, *Chin. Sci. Bull.* **59**, 125-132 (2014). [arXiv:1301.6246]
- [14] Y. Y. Fan, Z. J. Xiao, R. M. Wang and B. Z. Li, The $B \rightarrow D^{(*)}\ell\nu_\ell$ decays in the pQCD approach with the Lattice QCD input, *Sci. Bull.* **60**, 2009-2015 (2015). [arXiv:1505.07169]
- [15] T. Kurimoto, H. N. Li and A. I. Sanda, $B \rightarrow D^{(*)}$ form-factors in perturbative QCD, *Phys. Rev. D* **67**, 054028 (2003). [hep-ph/0210289]
- [16] F. Zuo, Z. H. Li and T. Huang, Form Factor for $B \rightarrow D\ell\bar{\nu}$ in Light-Cone Sum Rules With Chiral Current Correlator, *Phys. Lett. B* **641**, 177-182 (2006). [hep-ph/0606187]
- [17] F. Zuo and T. Huang, B_c (B) $\rightarrow D\ell\bar{\nu}$ form-factors in light-cone sum rules and the D -meson distribution amplitude, *Chin. Phys. Lett.* **24**, 61-64 (2007). [hep-ph/0611113]
- [18] H. B. Fu, X. G. Wu, H. Y. Han, Y. Ma and T. Zhong, $|V_{cb}|$ from the semileptonic decay $B \rightarrow D\ell\bar{\nu}_\ell$ and the properties of the D -meson distribution amplitude, *Nucl. Phys. B* **884**, 172-192 (2014). [arXiv:1309.5723]
- [19] Y. Zhang, T. Zhong, X. G. Wu, K. Li, H. B. Fu and T. Huang, Uncertainties of the $B \rightarrow D$ transition form factor from the D -meson leading-twist distribution amplitude, *Eur. Phys. J. C* **78**, 76 (2018). [arXiv:1709.02226]
- [20] Y. M. Wang, Y. B. Wei, Y. L. Shen and C. D. Lü, Perturbative corrections to $B \rightarrow D$ form factors in QCD, *JHEP* **06**, 062 (2017). [arXiv:1701.06810]
- [21] J. Gao, T. Huber, Y. Ji, C. Wang, Y. M. Wang and Y. B. Wei, $B \rightarrow D\ell\nu_\ell$ form factors beyond leading power and extraction of $|V_{cb}|$ and $R(D)$, *JHEP* **05**, 024 (2022). [arXiv:2112.12674]
- [22] T. Zhong, Y. Zhang, X. G. Wu, H. B. Fu and T. Huang, The ratio $\mathcal{R}(D)$ and the D -meson distribution amplitude, *Eur. Phys. J. C* **78**, 937 (2018). [arXiv:1807.03453]
- [23] D. L. Yao, P. Fernandez-Soler, F. K. Guo and J. Nieves, New parametrization of the form factors in $\bar{B} \rightarrow D\ell\bar{\nu}_\ell$ decays, *Phys. Rev. D* **101**, 034014 (2020). [arXiv:1906.00727]
- [24] J. A. Bailey *et al.* [MILC], $B \rightarrow D\ell\nu$ form factors at nonzero recoil and $|V_{cb}|$ from 2+1-flavor lattice QCD, *Phys. Rev. D* **92**, 034506 (2015). [arXiv:1503.07237]
- [25] G. M. de Divitiis, E. Molinaro, R. Petronzio and N. Tantalo, Quenched lattice calculation of the $B \rightarrow D\ell\nu$ decay rate, *Phys. Lett. B* **655**, 45-49 (2007). [arXiv:0707.0582]
- [26] M. Okamoto, C. Aubin, C. Bernard, C. E. DeTar, M. Di Pierro, A. X. El-Khadra, S. Gottlieb, E. B. Gregory, U. M. Heller and J. Hetrick, *et al.* Semileptonic $D \rightarrow \pi/K$ and $B \rightarrow \pi/D$ decays in 2+1 flavor lattice QCD, *Nucl. Phys. B Proc. Suppl.* **140**, 461-463 (2005). [arXiv:hep-lat/0409116]
- [27] S. Hashimoto, A. X. El-Khadra, A. S. Kronfeld, P. B. Mackenzie, S. M. Ryan and J. N. Simone, Lattice QCD calculation of $\bar{B} \rightarrow D\ell\bar{\nu}$ decay form-factors at zero recoil, *Phys. Rev. D* **61**, 014502 (1999). [hep-ph/9906376]
- [28] C. Bernard, C. E. DeTar, M. Di Pierro, A. X. El-Khadra, R. T. Evans, E. D. Freeland, E. Gamiz, S. Gottlieb, U. M. Heller and J. E. Hetrick, *et al.* The $\bar{B} \rightarrow D^*\ell\bar{\nu}$ form factor at zero recoil from three-flavor lattice QCD: A Model independent determination of $|V_{cb}|$, *Phys. Rev. D* **79**, 014506 (2009). [arXiv:0808.2519]
- [29] H. Na *et al.* [HPQCD], $B \rightarrow D\ell\nu$ form factors at nonzero recoil and extraction of $|V_{cb}|$, *Phys. Rev. D* **92** no.5, 054510 (2015) [erratum: *Phys. Rev. D* **93**, 11]. [arXiv:1505.03925]
- [30] T. Kaneko *et al.* [JLQCD], $B \rightarrow D^{(*)}\ell\nu$ form factors from lattice QCD with relativistic heavy quarks, *PoS LATTICE2019*,139(2019). [arXiv:1912.11770]
- [31] B. Y. Cui, Y. K. Huang, Y. L. Shen, C. Wang and Y. M. Wang, Precision calculations of $B_{d,s} \rightarrow \pi, K$ decay form factors in soft-collinear effective theory, *JHEP* **03**, 140 (2023). [arXiv:2212.11624]
- [32] B. Y. Cui, Y. K. Huang, Y. M. Wang and X. C. Zhao, Shedding new light on $R(D_{(s)}^{(*)})$ and $|V_{cb}|$ from semileptonic $B_{(s)} \rightarrow D_{(s)}^{(*)}\ell\bar{\nu}_\ell$ decays, *Phys. Rev. D* **108**, L071504 (2023). [arXiv:2301.12391]
- [33] S. M. Hu, W. Wang, J. Xu and S. Zhao, Accessing the subleading-twist B -meson light-cone distribution amplitude with large-momentum effective theory, *Phys. Rev. D* **109**, 034001 (2024). [arXiv:2308.13977]
- [34] W. Wang, Y. M. Wang, J. Xu and S. Zhao, B -meson light-cone distribution amplitude from Euclidean quantities, *Phys. Rev. D* **102**, 011502 (2020). [arXiv:1908.09933]
- [35] J. Gao, C. D. Lü, Y. L. Shen, Y. M. Wang and Y. B. Wei, Precision calculations of $B \rightarrow V$ form factors from soft-collinear effective theory sum rules on the light-cone, *Phys. Rev. D* **101**, 074035 (2020). [arXiv:1907.11092]
- [36] Y. L. Shen, Y. M. Wang and Y. B. Wei, Precision calculations of the double radiative bottom-meson decays in soft-collinear effective theory, *JHEP* **12**, 169 (2020). [arXiv:2009.02723]
- [37] X. G. Wu and T. Huang, An Implication on the Pion Distribution Amplitude from the Pion-Photon Transition Form Factor with the New BABAR Data, *Phys. Rev. D* **82**, 034024 (2010). [arXiv:1005.3359]

- [38] X. G. Wu and T. Huang, Constraints on the Light Pseudoscalar Meson Distribution Amplitudes from Their Meson-Photon Transition Form Factors, *Phys. Rev. D* **84**, 074011 (2011). [arXiv:1106.4365]
- [39] T. Huang, T. Zhong and X. G. Wu, Determination of the pion distribution amplitude, *Phys. Rev. D* **88**, 034013 (2013). [arXiv:1305.7391]
- [40] T. Huang, B. Q. Ma and Q. X. Shen, Analysis of the pion wave function in light cone formalism, *Phys. Rev. D* **49**, 1490-1499 (1994). [hep-ph/9402285]
- [41] X. G. Wu, T. Huang and T. Zhong, Information on the Pion Distribution Amplitude from the Pion-Photon Transition Form Factor with the Belle and BABAR Data, *Chin. Phys. C* **37**, 063105 (2013). [arXiv:1206.0466]
- [42] F. G. Cao and T. Huang, Large corrections to asymptotic $F_{\eta_c\gamma}$ and $F_{\eta_b\gamma}$ in the light cone perturbative QCD, *Phys. Rev. D* **59**, 093004 (1999). [hep-ph/9711284]
- [43] X. G. Wu and T. Huang, Pion electromagnetic form-factor in the K_T factorization formulae, *Int. J. Mod. Phys. A* **21**, 901-904 (2006). [hep-ph/0507136]
- [44] X. G. Wu and T. Huang, Kaon Electromagnetic Form-Factor within the k_T Factorization Formalism and It's Light-Cone Wave Function, *JHEP* **04**, 043 (2008). [arXiv:0803.4229]
- [45] E. P. Wigner, *On unitary representations of the inhomogeneous lorentz group*, *Annals Math.* **40**, 149-204 (1939).
- [46] H. J. Melosh, *Quarks: currents and constituents*, *Phys. Rev. D* **9**, 1095 (1974).
- [47] L. A. Kondratyuk and M. V. Terentev, The scattering problem for relativistic systems with fixed number of particles, *Sov. J. Nucl. Phys.* **31**, 561, ITEP-48-1979 (1980).
- [48] C. G. Boyd, B. Grinstein and R. F. Lebed, Constraints on form-factors for exclusive semileptonic heavy to light meson decays, *Phys. Rev. Lett.* **74**, 4603-4606 (1995). [hep-ph/9412324]
- [49] T. Huang, Z. H. Li and X. Y. Wu, Improved approach to the heavy to light form-factors in the light cone QCD sum rules, *Phys. Rev. D* **63**, 094001 (2001).
- [50] P. Ball, Theoretical update of pseudoscalar meson distribution amplitudes of higher twist: The Nonsinglet case, *JHEP* **01** 010 (1999). [hep-ph/9812375]
- [51] N. Isgur and M. B. Wise, Weak Decays of Heavy Mesons in the Static Quark Approximation, *Phys. Lett. B* **232**, 113-117 (1989).
- [52] N. Isgur and M. B. Wise, Weak transition form factors between heavy mesons, *Phys. Lett. B* **237**, 527-530 (1990).
- [53] T. Huang and X. G. Wu, A Model for the twist-3 wave function of the pion and its contribution to the pion form-factor, *Phys. Rev. D* **70**, 093013 (2004). [hep-ph/0408252]
- [54] T. Zhong, Z. H. Zhu, H. B. Fu, X. G. Wu and T. Huang, Improved light-cone harmonic oscillator model for the pionic leading-twist distribution amplitude, *Phys. Rev. D* **104** 016021 (2021). [arXiv:2102.03989]
- [55] T. Zhong, H. B. Fu and X. G. Wu, Investigating the ratio of CKM matrix elements $|V_{ub}|/|V_{cb}|$ from semileptonic decay $B_s^0 \rightarrow K^-\mu^+\nu_\mu$ and kaon twist-2 distribution amplitude, *Phys. Rev. D* **105** 116020 (2022). [arXiv:2201.10820]
- [56] H. J. Tian, H. B. Fu, T. Zhong, Y. X. Wang and X. G. Wu, The rare decay $B^+ \rightarrow K^+\ell^+\ell^-(\nu\bar{\nu})$ under the QCD sum rules approach, arXiv:2411.12141.
- [57] D. Huang, T. Zhong, H. B. Fu, Z. H. Wu, X. G. Wu and H. Tong, $K_0^*(1430)$ twist-2 distribution amplitude and $B_s, D_s \rightarrow K_0^*(1430)$ transition form factors, *Eur. Phys. J. C* **83** 680 (2023). [arXiv:2211.06211]
- [58] Z. H. Wu, H. B. Fu, T. Zhong, D. Huang, D. D. Hu and X. G. Wu, $a_0(980)$ -meson twist-2 distribution amplitude within the QCD sum rules and investigation of $D \rightarrow a_0(980)(\rightarrow \eta\pi)e^+\nu_e$, *Nucl. Phys. A* **1036**, 122671 (2023). [arXiv:2211.05390]
- [59] Y. L. Yang, Y. X. Wang, H. B. Fu, T. Zhong and Y. L. Song, Scrutinizing B^0 -meson flavor changing neutral current decay into scalar $K_0^*(1430)$ meson with $b \rightarrow s\ell^+\ell^-(\nu\bar{\nu})$ transition, arXiv:2410.09363.
- [60] Y. L. Yang, H. J. Tian, Y. X. Wang, H. B. Fu, T. Zhong, S. Q. Wang and D. Huang, Probing $|V_{cs}|$ and lepton flavor universality through $D \rightarrow K_0^*(1430)\ell\nu_\ell$ decays, *Phys. Rev. D* **110**, 116030 (2024). [arXiv:2409.01512]
- [61] H. B. Fu, X. G. Wu, W. Cheng and T. Zhong, ρ -meson longitudinal leading-twist distribution amplitude within QCD background field theory, *Phys. Rev. D* **94** 074004 (2016). [arXiv:1607.04937]
- [62] D. D. Hu, X. G. Wu, L. Zeng, H. B. Fu and T. Zhong, Improved light-cone harmonic oscillator model for the ϕ -meson longitudinal leading-twist light-cone distribution amplitude and its effects to $D_s^+ \rightarrow \phi\ell^+\nu_\ell$, *Phys. Rev. D* **110** 056017 (2024). [arXiv:2403.10003]
- [63] X. Q. Li, T. Huang and Z. C. Zhang, The Contribution of Color Octet Current \times Color Octet Current to D Decays, *Z. Phys. C* **42**, 99 (1989).
- [64] X. H. Guo and T. Huang, Hadronic wave functions in D and B decays, *Phys. Rev. D* **43**, 2931-2938 (1991).
- [65] Y. J. Sun, X. G. Wu, F. Zuo and T. Huang, The Cross section of the process $e^+e^- \rightarrow J/\psi + \eta_c$ within the QCD light-cone sum rules, *Eur. Phys. J. C* **67**, 117-123 (2010). [arXiv:0911.0963]
- [66] S. Navas *et al.* [Particle Data Group], Review of particle physics, *Phys. Rev. D* **110** 030001 (2024).
- [67] P. Gelhausen, A. Khodjamirian, A. A. Pivovarov and D. Rosenthal, Decay constants of heavy-light vector mesons from QCD sum rules, *Phys. Rev. D* **88**, 014015 (2013). [arXiv:1305.5432]
- [68] K. Binder (ed.), 'Monte Carlo Methods in Statistical Physics', Springer, Berlin 1986.
- [69] Chris Sherlock, Gareth Roberts, Optimal scaling of the random walk Metropolis on elliptically symmetric unimodal targets, [arXiv:0909.0856]
- [70] R. H. Li, C. D. Lu and H. Zou, The $B(B_s) \rightarrow D_{(s)P}, D_{(s)}^*V, D_{(s)}^*P$ and $D_{(s)}^*V$ decays in the perturbative QCD approach, *Phys. Rev. D* **78**, 014018 (2008). [arXiv:0803.1073]
- [71] H. N. Li and B. Melic, Determination of heavy meson wave functions from B decays, *Eur. Phys. J. C* **11**, 695-702 (1999). [hep-ph/9902205]
- [72] N. Dhiman, H. Dahiya, C. R. Ji and H. M. Choi, Twist-2 Pseudoscalar and Vector Meson Distribution Amplitudes in Light-Front Quark Model with Exponential-type Confining Potential, *Phys. Rev. D* **100**, 014026 (2019). [arXiv:1902.09160]
- [73] T. Zhong, D. Huang and H. B. Fu, Revisiting D -meson twist-2, 3 distribution amplitudes, *Chin. Phys. C* **47**, 053104 (2023). [arXiv:2212.04641]
- [74] A. Bharucha, D. M. Straub and R. Zwicky, $B \rightarrow V\ell^+\ell^-$ in the Standard Model from light-cone sum rules, *JHEP* **08**, 098 (2016). [arXiv:1503.05534]

- [75] A. Bharucha, T. Feldmann and M. Wick, Theoretical and Phenomenological Constraints on Form Factors for Radiative and semileptonic B -Meson Decays, *JHEP* **09**, 090 (2010). [[arXiv:1004.3249](#)]
- [76] P. A. Zyla *et al.* [Particle Data Group], Review of Particle Physics, *PTEP* **2020**, 083C01 (2020)